

# Performance Evaluation of Three-Phase Grid Connected Inverter with Various Control Methods

Ekrem Demir, Ozan Gulbudak, Mustafa Gokdag


**Abstract**— Grid-connected inverters, one of the widely used power systems to benefit from renewable energy systems, play an important role. According to the TS EN 50160 standard specified in our country, the total harmonic distortion value of the grid current of the grid-connected inverters must be below 5%. Various filter models are used between the inverter and the grid to suppress the harmonic distortions of the current generated from the inverters and to keep the THD value of the grid current below the specified standard. Among these filter models, L and LCL filter models are widely used. Among these filters, the LCL filter suppresses harmonics more than the L filter. In addition to the THD value of the mains current being below the desired standard, the dynamics of the system should be regular. Various feedback strategies (Control methods) are available to regulate the dynamics of grid-connected systems. Linear controllers, non-linear controllers and predictive controllers play an important role in controlling grid-connected inverter systems. In this study, different control strategies are investigated to analyze the performance of the grid-tied inverter equipped with an LCL filter. Then, simulation studies were carried out by applying traditional Proportional-Integral-Derivative (PID) control, Sliding Mode Control (SMC) and Model Predictive Control (MPC) method to grid-connected LCL filtered inverter. Simulation studies were carried out using MATLAB and theoretical concepts were verified by simulation studies.

**Index Terms**—PID control, Sliding mode control, Model predictive control, grid-tide inverter


## I. INTRODUCTION

RECENTLY, Renewable energy production system(REPS) applications have increased due to the negative effects and costs of fossil fuels(health cost and environmental cost) on the environment in terms of energy production systems [1].


EKREM DEMİR, is with Department of Electrical Engineering University of Karabuk University, Karabuk, Turkey, (e-mail: [edemir@karabuk.edu.tr](mailto:edemir@karabuk.edu.tr)).

 <https://orcid.org/0000-0001-7882-9634>

OZAN GULBUDAK, is with Department of Electrical Engineering University of Karabuk University, Karabuk, Turkey, (e-mail: [ozangulbudak@karabuk.edu.tr](mailto:ozangulbudak@karabuk.edu.tr)).

 <https://orcid.org/0000-0001-9517-3630>

MUSTAFA GOKDAĞ, is with Department of Electrical Engineering University of Karabuk University, Karabuk, Turkey, (e-mail: [mgokdag@karabuk.edu.tr](mailto:mgokdag@karabuk.edu.tr)).

 <https://orcid.org/0000-0001-5589-2278>

Manuscript received Sep 13, 2022; accepted Feb 9, 2023.

DOI: [10.17694/bajece.1174749](https://doi.org/10.17694/bajece.1174749)

Three-phase grid-connected inverter topology is depicted in Fig. 1. [2], [3].

Various filters and control methods are used to suppress the harmonics of the inverter's output current connected to the grid. Among the filters, the L filter is not preferred to be used due to its high cost and slow system dynamic response in high power applications. Furthermore, the use of L filter may suffer from poor harmonic rejection capability. Thus, the LCL filter is usually preferred since third-order attenuation is achieved resulting in improved power quality [4], [5].

In the literature, several control methods have been reported to control the grid-connected system. In traditional control routine, a piece-wise modulator combined with linear controller such as PID controller is used. The traditional strategy offers a reasonable energy conversion operation. However, the dynamic response degraded due to the slow dynamics of the modulator [6], [7]. The other critical aspect of the traditional method, the feedback design is based on the linear relationship between input-output variables (basically pole-zero based transfer function). The controller parameters are tuned such that a decent closed-loop performance is achieved. However, the controller parameters (such as proportional or integral coefficients) are fixed during the operation, thus a deviation from the operating point negatively influences the reference tracking performance. Due to this unpleasant characteristics, nonlinear control strategies are desirable to improve transient performance of the system. Nonlinear control methods overcome stated problems since they have capability to adapt the new operating conditions [8].

This paper presents the performance evaluation of different control strategies for grid-connected inverter. Three feedback methods are considered as case studies: PID controller, SMC and MPC. The performance evaluation is conducted regarding various evaluation metrics. Among aforementioned control methods, MPC strategy is very promising. MPC provides a rapid response to the load perturbations while ensuring the closed-loop stability. Mathematical concepts are verified by the simulation works, and each control method is tested considering real-case test scenarios.

## II. SYSTEM MODEL

The three-phase voltage source inverter (VSI), see Fig. 1, has eight permissible switching combinations. Each discrete semiconductor device can have two discrete values (1 or 0). There are two switching limitations in VSI operation. The

switching devices on the same VSI leg cannot be simultaneously conducted due to dc-bus short circuit. Table I summarize allowable switching positions for VSI [9].

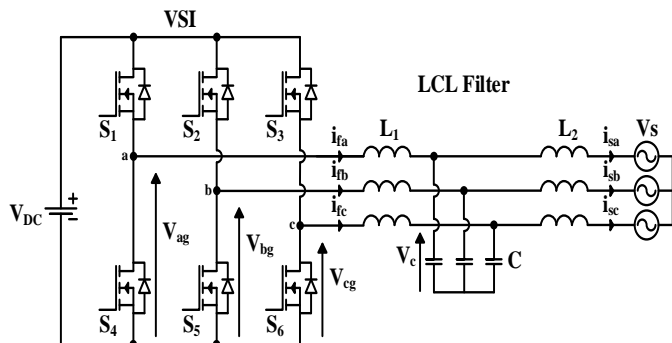


Fig. 1. The grid-connected VSI with LCL-type filter [3]

TABLE I ALLOWABLE SWITCH POSITIONS OF INVERTER LEGS [9]

$S_a$	$S_b$	$S_c$
0	0	0
1	0	0
1	1	0
0	1	0
0	1	1
0	0	1
1	0	1
1	1	1

A. Output Filter Model

Power converters are used to integrate most renewable energy systems with the electrical grid. In the grid-connected systems, an output filter is often used to reduce the harmonics of the grid current generated from power converters. These filters can take different structures such as L, LC, LCL filters [10], [11].

The L filter has a simple structure since it is a first-order filter. However, in order to reduce the harmonics of the mains current, a large inductance value L filter must be used. A filter of this value has disadvantages such as high cost and negative control time response [11], [12].

An LC filter has been proposed as an alternative to the L filter. Because the LC filter is a second order filter, it reduces the filter volume and increases attenuation for high frequencies. However, it has disadvantages such as the has of inrush currents in the output capacitance , a resonant frequency that amplify the mains current harmonics, and the instability caused by the direct connection of the capacitor in parallel to the electrical network [11], [13].

Although the LCL filter has a more difficult design due to having a third order filter compared to the L and LC filters, it offers better harmonic attenuation performance and lower cost to reduce the mains current harmonics [14]. In this work, LCL filter is used, and the design guideline [15] to determine LCL filter parameters is given in Fig. 2 [16]. Based on the algorithm presented in , the selected filter parameters are tabulated in Table 2.

TABLE II LCL FILTER PARAMETERS USED IN SIMULATION STUDY

LCL Filter Parameters		System Parameters	
Inverter side inductor	$L_i = 24.44 \text{ mH}$	One Phase Effective Voltage	$E_n = 220 \text{ V}$
Damping Resistor	$R_f = 1.1772 \Omega$	Active Power	$P = 2700 \text{ W}$
Capacitor Filter	$C_f = 8.88 \mu\text{F}$	DC link Voltage	$V_{DC} = 750 \text{ V}$
Grid side inductor	$L_g = 0.11 \text{ mH}$	Grid Frequency	$f_g = 50 \text{ Hz}$
Resonance angular velocity	$\omega_{res} = 32068 \text{ rad}$	Switching Frequency	$f_{sw} = 12.5 \text{ kHz}$
Resonance Frequency	$f_{res} = 5103 \text{ Hz}$	Attenuation Factor	$k_a = 0.2(\%20)$

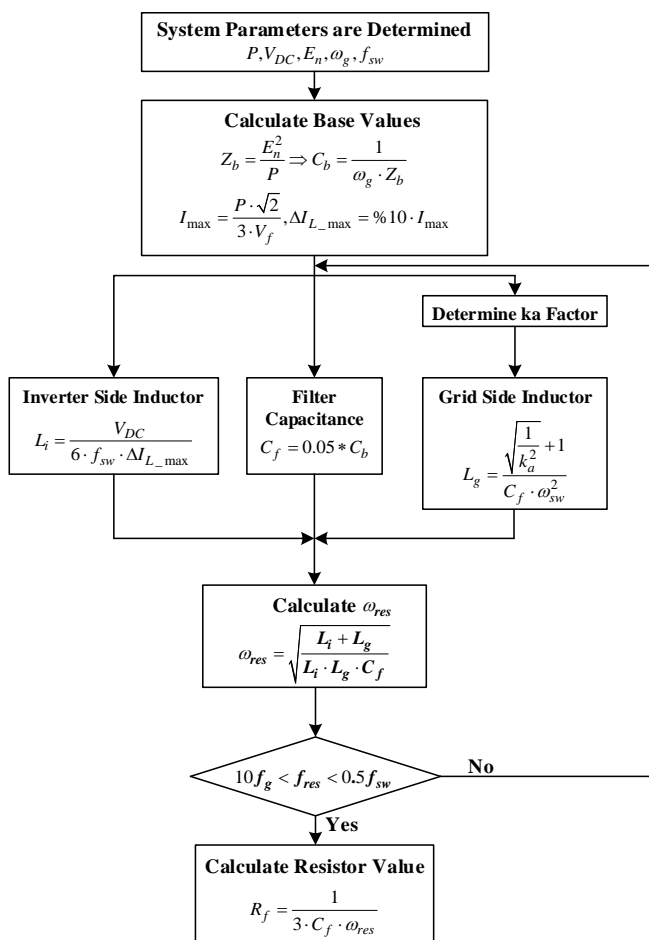


Fig. 2. Algorithm of LCL-filter [16]

III. CONTROL METHOD

This section presents feedback strategies to control the grid-connected VSI with LCL filter. Herein, three control methods are discussed by providing the mathematical models and design steps. Firstly, linear PID controller is discussed. Then, SMC and MPC methods will be explained.

A. Classic PID Control

The control system with feedback classic PID controller is given in Fig. 3. Where  $r$ ,  $e$ ,  $y$  are respectively reference, error and the output of the system that is controlled variable. Also, in the Fig. 3,  $G(s)$  represents the transfer function of the system to be controlled and  $C(s)$  represents the PID controller [17].

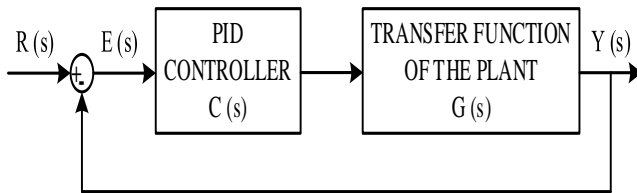


Fig. 3. The PID control block diagram of system [17]

The PID controller is used to reduce or eliminate the steady state error as well as improve the dynamic response [18]. The transfer function of the PID controller is given in the equation which is the below [19]:

$$C(s) = K_p + \frac{K_I}{s} + K_D s \tag{1}$$

Where,  $K_p$ ,  $K_I$ ,  $K_D$  represents the proportional, integral, and derivative gain of the PID controller controlling the system, respectively [19].

In this work, The PID control method compares the inductor current that is near grid with the desired reference current. Then it multiplies this error with the PID coefficients we have determined. Finally, it determines the status of the switches of the inverter system by comparing the obtained value with the carrier signal as shown in Fig. 4.

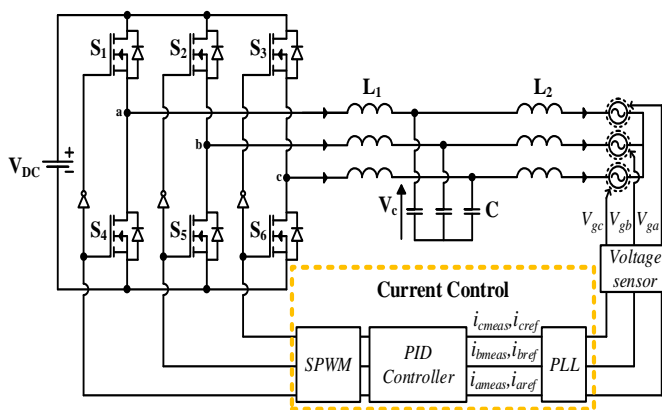


Fig. 4. Classic PID Control scheme for the grid connected VSI

B. Sliding-mode Control Sliding-mode control of grid-connected VSI

The sliding mode control (SMC) is a nonlinear feedback control strategy. SMC is an encouraging control strategy in power electronics applications where the control of multiple control objectives is required. The state variables usually are defined as trajectory error, and the control of the state variables is achieved by rotating the sliding line. Due to the resonance problem of the LCL-type filter, the sliding surface function can

be properly selected [20]. In this work, the sliding surface function is formed by the grid-side current, capacitor voltage, and time-derivative of the capacitor voltage.

The dynamic model of the system is given by

$$L_1 \frac{di_f}{dt} = v_g - v_c \tag{2}$$

$$L_2 \frac{di_s}{dt} = v_c - v_s \tag{3}$$

$$C \frac{dv_c}{dt} = i_f - i_s \tag{4}$$

In (1)-(3),  $v_g = [S_1 v_{dc} \ S_2 v_{dc} \ S_3 v_{dc}]$  with  $S_1, S_2, S_3 \in \{1, 0\}$  and  $S_3 \in \{1, 0\}$ ,  $i_f = [i_{fa} \ i_{fb} \ i_{fc}]$ . The input voltage  $v_g$  depends on the switching positions. The state variables are expressed as

$$x_1 = v_c - v_c^* \tag{5}$$

$$x_2 = \frac{dv_c}{dt} - \frac{dv_c^*}{dt} \tag{6}$$

$$x_3 = i_s - i_s^* \tag{7}$$

Where  $v_c = [v_{ca} \ v_{cb} \ v_{cc}]$ ,  $i_s = [i_{sa} \ i_{sb} \ i_{sc}]$ ,  $v_c^* = [v_{ca}^* \ v_{cb}^* \ v_{cc}^*]$  and  $i_s^* = [i_{sa}^* \ i_{sb}^* \ i_{sc}^*]$ . The vector  $v_c^*$  denotes the capacitor voltage reference and  $i_s^*$  is the grid current reference.

From (4) and (5), the time-derivative of  $x_1$  equals  $x_2$  ( $\dot{x}_1 = x_2$ ).

Conceptually, the SMC aims to control the capacitor voltage and the grid current. By using the state variables defined in (4)-(6), the sliding surface function is defined as

$$S = \lambda x_1 + x_2 + \sigma x_3 \tag{8}$$

In (7),  $\lambda$  and  $\sigma$  are the time-invariant parameters that define the moving speed of the sliding line. The parameter  $\lambda$  is the tuning term of the capacitor voltage control term. Fundamentally, it manages the importance of capacitor voltage control. The parameter  $\sigma$  is the constant gain of the instantaneous grid current error. The grid current control performance can be tuned by adjusting  $\sigma$ . Thus, the selection of  $\lambda$  and  $\sigma$  are quite important since they have a noticeable influence on the closed-loop dynamics. During the sliding mode, the sliding function equals zero ( $S = 0$ ). In this case, the state variable lies on the sliding line, and they move to the origin of the phase-plane. To ensure the asymptotical stability, the SMC stability condition is considered.

$$S \dot{S} < 0 \tag{9}$$

On the authority of (5), the state variable error converges to zero if the condition  $S \dot{S} < 0$  is satisfied. The time-derivative of (4) results

$$\dot{S} = \lambda \dot{x}_1 + \dot{x}_2 + \sigma \dot{x}_3 \quad (10)$$

By managing (1) and (2), the following expressions can be obtained.

$$\frac{di_f}{dt} = \frac{1}{L_1}(v_g - v_c) \quad (11)$$

$$\frac{di_s}{dt} = \frac{1}{L_2}(v_c - v_s) \quad (12)$$

By applying the same procedure, the time-derivative of the capacitor voltage is given by

$$\frac{dv_c}{dt} = \frac{1}{L_2}(i_f - i_s) \quad (13)$$

By substituting (12) into (2),  $x_2$  results as:

$$x_2 = \frac{1}{C}(i_f - i_s) - \frac{dv_c^*}{dt} \quad (14)$$

The time-derivative of  $x_2$  can be determined by taking a derivative of (13). Hence, the derivative term of  $x_2$  is expressed as

$$\dot{x}_2 = \frac{1}{C} \left( \frac{di_f}{dt} - \frac{di_s}{dt} \right) - \frac{d^2v_c^*}{dt^2} \quad (15)$$

Using (10) and (11), the expression (14) becomes as follows:

$$\dot{x}_2 = \frac{1}{L_1 C} v_g - v_c \left( \frac{1}{L_1 C} + \frac{1}{L_2 C} \right) + \frac{1}{L_1 C} v_s - \frac{d^2v_c^*}{dt^2} \quad (16)$$

The time derivative of  $x_3$  is expressed as

$$\dot{x}_3 = \frac{di_s}{dt} - \frac{di_s^*}{dt} \quad (17)$$

To implement the SMC method, a proper control input should be defined. The control input  $u$  is defined as

$$u = -\text{sign}(S) \quad (18)$$

The control input has the value of 1 when  $S > \Psi$ , and it holds the value of -1 when  $S > -\Psi$ . As aforementioned before, S refers to the sliding surface defined in (7). The control input is determined in a hysteresis-based mechanism. In this work, the SMC method is implemented in the discrete-time domain. To derive the sampled model of the system, numerical discretization methods can be applied. In this work, the Forward Euler method is used to derive the discrete-time model of the system. By using the Forward Euler method and (1)-(3), the sampled model of the system can be expressed as

$$i_f(k+1) = i_f(k) + \frac{T_s}{L_1}(v_g(k) - v_c(k)) \quad (19)$$

$$i_s(k+1) = i_s(k) + \frac{T_s}{L_2}(v_c(k) - v_s(k)) \quad (20)$$

$$v_c(k+1) = v_c(k) + \frac{T_s}{C}(i_f(k) - i_s(k)) \quad (21)$$

The working principle of the SMC method for the grid connected VSI is illustrated in Fig. 5.

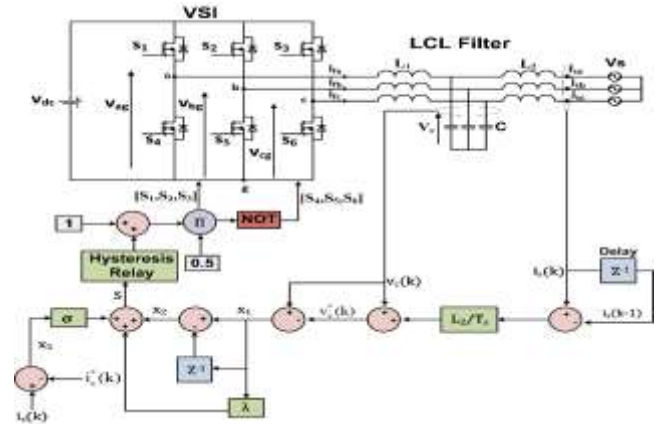


Fig. 5. The SMC scheme for the grid-connected VSI

C. Model Predictive Control

The MPC is a nonlinear control strategy. This control method has been applied in power electronics applications since 1980. Recently, with the improvement of the performance of microprocessors, the interest in the MPC algorithm has increased even more. The main feature of this algorithm, whose working principle is graphically illustrated in Fig. 6, is to predict the future behavior of predefined control variables on the time horizon with a certain sampling time. It is then to use the estimated variables to obtain the optimal switching state by minimizing the cost function [21]–[24].

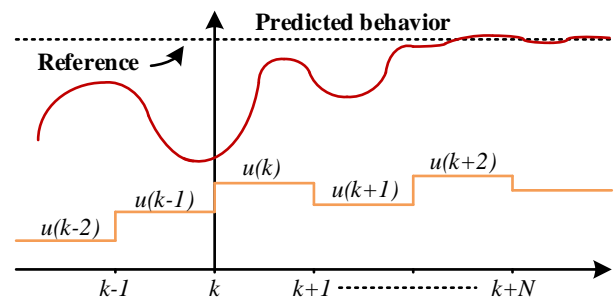


Fig. 6. Working principle of MPC [21]

For power electronics inverters, the MPC can be designed using the following steps [25]:

- 1) Measuring currents and voltages of materials required for modelling.
- 2) Generating all possible switching states and modeling of the power inverter which these states are identifying relation to the input or output voltages or currents.

- 3) Defining a cost function that represents the desired behavior of the system.
- 4) Obtaining discrete-time models that allow one to predict the future behavior of the variables to be controlled.

As a first step in this study, the dynamic model of the system in the  $t$  domain was obtained by applying the ambient current method. The dynamic model of the LCL filter is given as:

$$-V_{in} + L_1 \frac{dI_0}{dt} + I_C R + V_C = 0 \quad (22)$$

$$C \frac{dV_C}{dt} = I_0 - I_g \quad (23)$$

$$-V_C - I_C R + L_2 \frac{dI_g}{dt} + V_g = 0 \quad (24)$$

Then, discrete time models are obtained that allow to predict the behavior of the variables to be controlled for all possible switching states. Numerical methods (such as Forward Euler method or Tustin strategy) can be used to formulate the discrete-time model of the system. The discrete-time model of the dynamical model of the system given above is given as follows:

$$-V_{in}(k) + L_1 \left( \frac{I_0(k+1) - I_0(k)}{T_s} \right) + I_C(k)R + V_C(k) = 0 \quad (25)$$

$$C \left( \frac{V_C(k+1) - V_C(k)}{T_s} \right) = I_0(k+1) - I_g(k) \quad (26)$$

$$-V_C(k+1) - I_C(k)R + L_2 \left( \frac{I_g(k+1) - I_g(k)}{T_s} \right) + V_g(k) = 0 \quad (27)$$

The cost function is calculated for each estimate. Calculated cost functions are compared between them. Finally, the switching state that minimizes this function is chosen among them. The cost function of the system is given as:

$$g = |I_{ref} - I_{pre}|^2 \quad (28)$$

The working principle of the MPC method for the grid connected VSI is illustrated in Fig. 7.

#### IV. SIMULATION RESULTS

This section presents the simulation and comparison results. Performance evaluation is performed regarding steady-state performance, transient characteristics and harmonic suppression capability.

##### A. Steady-Performance

The steady states and the total harmonic distortion of the grid side current and voltage with respectively PID, SMC and MPC control methods applied are given in Fig. 8, Fig. 9 and Fig. 10. When using the respectively PID controller, SMC and MPC, FFT analysis on the grid current yields a THD value of 6.15%, 6.22% and 1.70% as shown in Fig. 8 (b), Fig. 9 (b) and Fig. 10 (b). As a result, it has been observed that if the MPC method is applied to the system, the system suppresses the harmonics of the mains current better and the mains current has a more stable structure compared to other control methods.

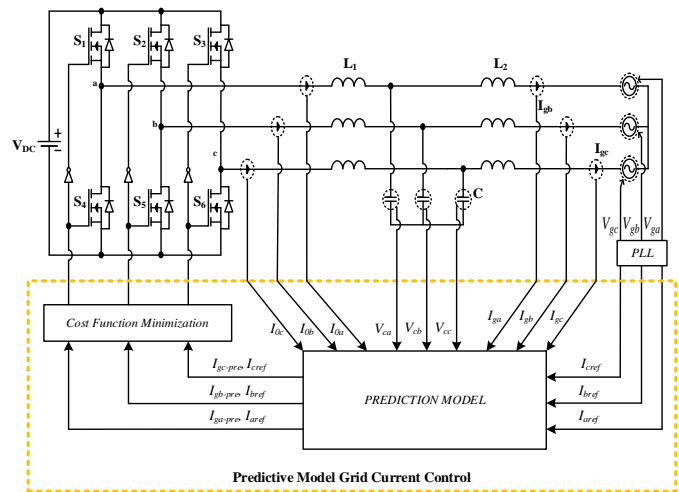


Fig. 7. The MPC scheme for the grid-connected VSI

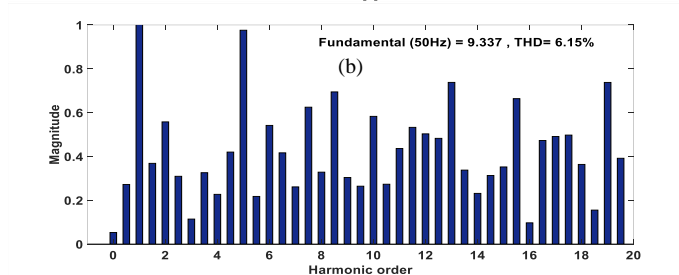
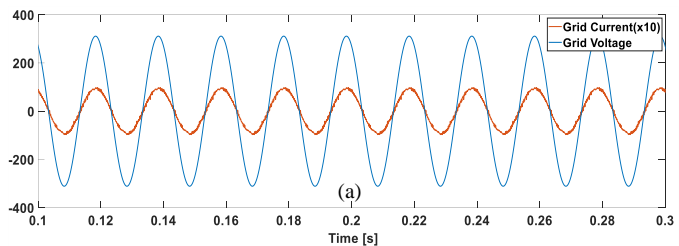


Fig. 8. For PID control method (a) steady-state results of grid currents and voltages and (b) FFT analysis of the grid current

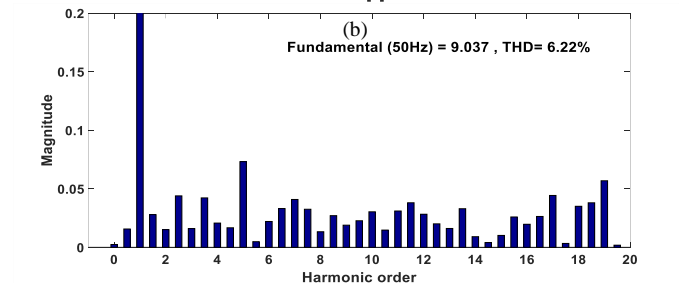
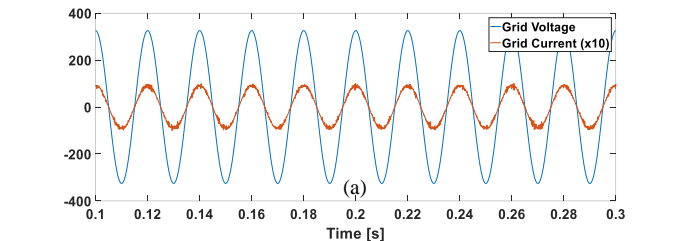


Fig. 9. For SMC control method (a) steady-state results of grid currents and voltages and (b) FFT analysis of the grid current



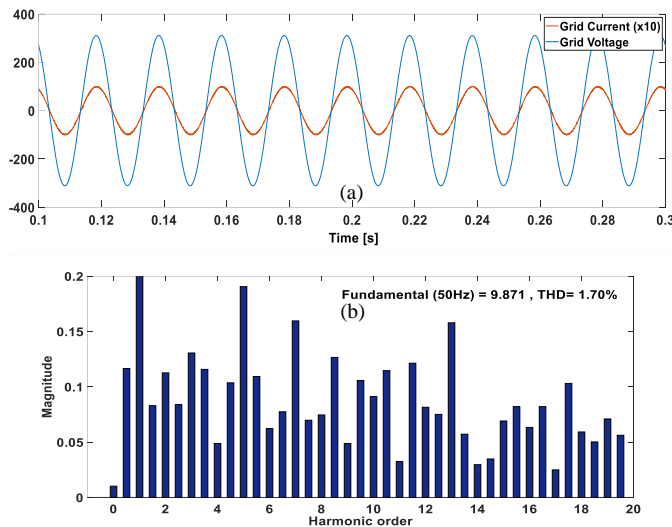


Fig. 10. For MPC control method (a) steady-state results of grid currents and voltages and (b) FFT analysis of the grid current

The steady states of the inverter side current and capacitor voltage with the application of the specified control methods to the system are given in Fig. 11 and Fig. 12. In addition, THD results for mains and inverter side current and capacitor voltage as a result of applying the specified control methods to the system are given in TABLE III in tabular form.

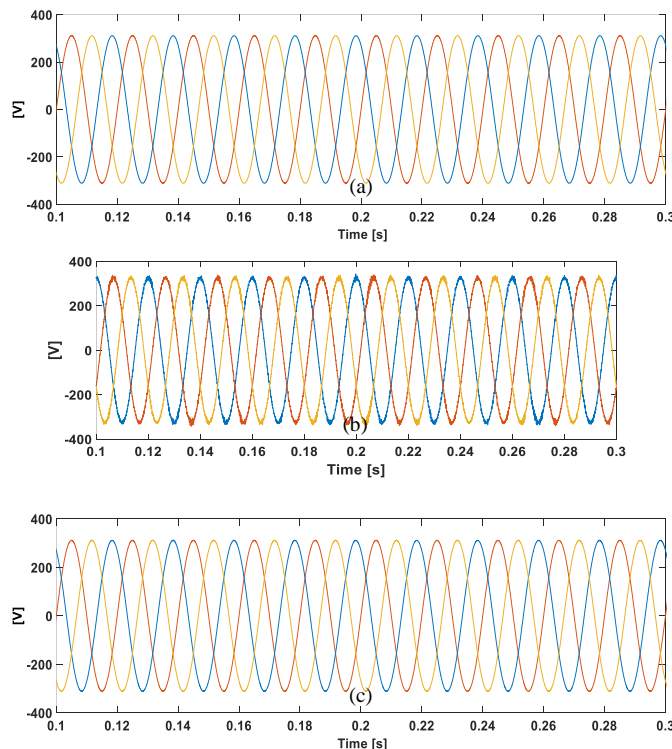


Fig. 11. For (a)PID, (b)SMC and (c) MPC methods steady-state results of capacitor voltages

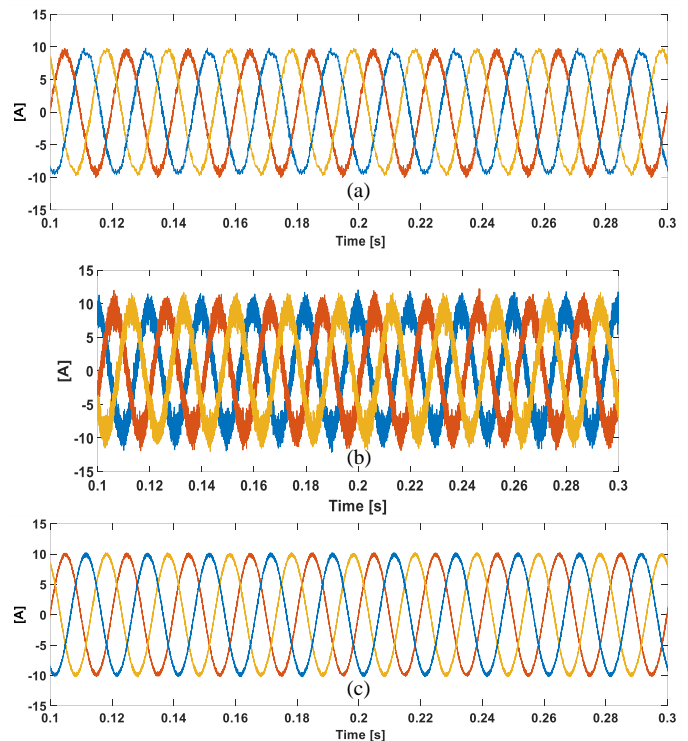


Fig. 12. For (a)PID, (b)SMC and (c) MPC methods steady-state results of inverter currents

TABLE III THD RESULTS FOR GRID SIDE, INVERTER SIDE CURRENT AND CAPACITOR VOLTAGE

Control Methods	THD of Grid Side Current	THD of Capacitor Voltage	THD of Inverter Side Current
PID	6,15 %	0,52 %	5,29 %
SMC	6,22 %	2,04 %	16,06 %
MPC	1,70 %	0,21 %	2,06 %

As seen in Fig. 8, Fig. 9, Fig. 10, Fig. 11, Fig. 12 and TABLE III, when the MPC method is applied to the system, it has been observed that it gives less THD than other methods. Moreover, it has been the inverter and grid current and capacitor voltage have a more stable structure.

**B. Transient-Performance**

During normal conditions, a step change is applied by switching the current mains current reference from 10A to 20A in 0.4 seconds using the PID, SMC and MPC control methods, respectively. Then, the transient performance of the grid current and voltage, capacitor voltage, and current on the inverter side is investigated.

Figure 11 (a), (b) and (c) show the simulation results of the transient response of measured grid current and voltage as a result of the change in reference current using the respective control methods, respectively. If these three methods are applied to the system, it has been observed that the MPC method reaches the desired reference current value in a shorter time compared to the SMC method and the SMC method compared to the PID control method. In other words, temporarily, it has been observed that the MPC method

responds faster to reach the desired reference value compared to other methods.

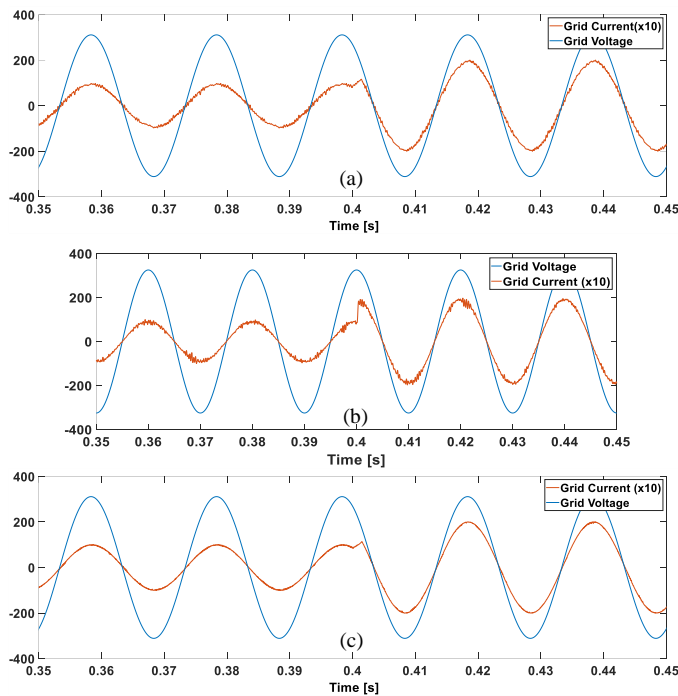


Fig. 13. For (a)PID, (b)SMC and (c) MPC methods transient results of grid currents and voltages

Figure 12 (a), (b) and (c) show the simulation results of the transient response of capacitor voltage as a result of the change in reference current using the respective control methods, respectively. In the case of MPC method is applied, it has been observed that the capacitor voltage is closer to the mains voltage compared to other control methods.

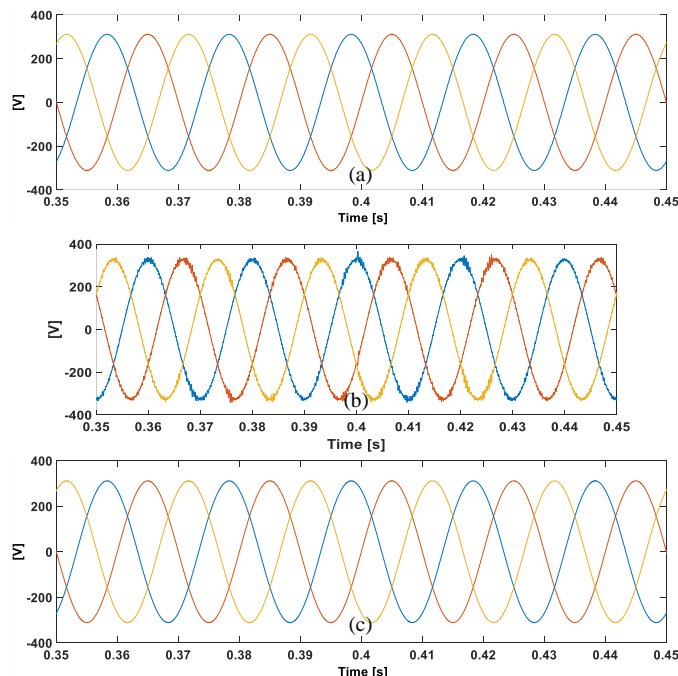


Fig. 14. For (a)PID, (b)SMC and (c) MPC methods transient results of capacitor voltages

Figure 13 (a), (b) and (c) show the simulation results of the transient response of inverter side current as a result of the change in reference current using the respective control methods, respectively. It has been observed that if the MPC method is applied to the system, it responds faster to reach the desired reference value of the current on the inverter side compared to other control methods.

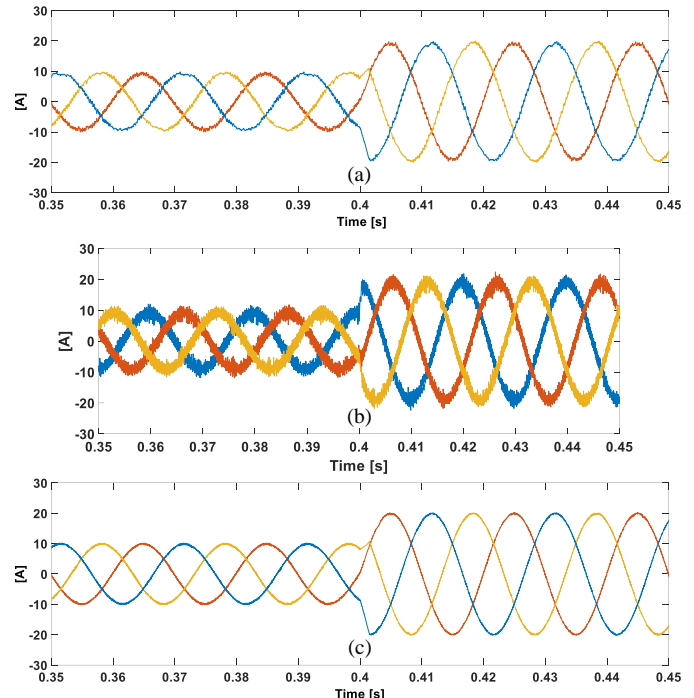


Fig. 15. For (a)PID, (b)SMC and (c) MPC methods transient results of inverter currents

### V. CONCLUSION

In this study, a three-phase grid-connected inverter system is designed. LCL filter is designed so that the mains current of the designed inverter system to be below 5% of THD value. In order for the grid current of the three-phase grid-connected inverter system to reach the desired reference current and the dynamic performance of the system to be good the control of the inverter system with different control methods has been carried out with a simulation study. First of these control methods, the PID control method, which is a linear control method, was applied to the inverter system. The PID coefficients of the PID control method are selected randomly. Secondly, the SMC method, which is a nonlinear control method, was applied to the system. For SMC control, the sliding surface function must be close to zero. Finally, the MPC control method, which is a predictive control method, has been applied to the inverter system. With this control method, the control of the system is achieved by estimating the future value of the measured current.

PID, SMC and MPC methods were applied to the designed LCL filtered grid-tied inverter system, respectively, and a simulation study was carried out. In the simulation study, firstly, steady state analysis was made, and it was seen that the system was stable in the case of applying the specified control

methods to the system. Secondly, FFT analysis of the inverter side, grid side current and capacitor voltage was performed, and it was observed that the MPC method was better than the other control methods in terms of THD value. Finally, transient analysis was performed, and it was observed that the measured current reached from 10A to 20A in a shorter time if the MPC method was applied compared to other control methods.

As a result, it has been seen that the MPC method gives better results than other control methods when applied to the inverter system. In future studies, the MPC method will be examined because it is easy to operate and control functions can be easily added to the cost function.

## REFERENCES

- [1] A. Demiroren and U. Yilmaz, "Analysis of change in electric energy cost with using renewable energy sources in Gökceada, Turkey: An island example," *Renew. Sustain. Energy Rev.*, vol. 14, no. 1, pp. 323–333, 2010, doi: 10.1016/j.rser.2009.06.030.
- [2] N. F. Guerrero-Rodríguez, A. B. Rey-Boué, and E. Reyes-Archundia, "Overview and comparative study of two control strategies used in 3-phase grid-connected inverters for renewable systems," *Renew. Energy Focus*, vol. 19–20, no. June, pp. 75–89, 2017, doi: 10.1016/j.ref.2017.05.007.
- [3] H. Zhang, J. Xian, J. Shi, S. Wu, and Z. Ma, "High Performance Decoupling Current Control by Linear Extended State Observer for Three-Phase Grid-Connected Inverter with an LCL Filter," *IEEE Access*, vol. 8, pp. 13119–13127, 2020, doi: 10.1109/ACCESS.2020.2965650.
- [4] M. Ben Saïd-Romdhane, M. W. Naouar, I. S. Belkhdja, and E. Monmasson, "Simple and systematic LCL filter design for three-phase grid-connected power converters," *Math. Comput. Simul.*, vol. 130, pp. 181–193, 2016, doi: 10.1016/j.matcom.2015.09.011.
- [5] C. Gurrola-Corral, J. Segundo, M. Esparza, and R. Cruz, "Optimal LCL-filter design method for grid-connected renewable energy sources," *Int. J. Electr. Power Energy Syst.*, vol. 120, no. 8, p. 105998, 2020, doi: 10.1016/j.ijepes.2020.105998.
- [6] K. Zeb et al., "A comprehensive review on inverter topologies and control strategies for grid connected photovoltaic system," *Renew. Sustain. Energy Rev.*, vol. 94, no. November 2017, pp. 1120–1141, 2018, doi: 10.1016/j.rser.2018.06.053.
- [7] H. Athari, M. Niroomand, and M. Ataei, "Review and Classification of Control Systems in Grid-tied Inverters," *Renew. Sustain. Energy Rev.*, vol. 72, no. October 2016, pp. 1167–1176, 2017, doi: 10.1016/j.rser.2016.10.030.
- [8] D. Menaga and V. Sankaranarayanan, "Performance comparison for grid connected photovoltaic system using sliding mode control," *J. King Saud Univ. - Eng. Sci.*, vol. 33, no. 4, pp. 276–283, 2021, doi: 10.1016/j.jksues.2020.04.012.
- [9] J. Rodriguez, P. Cortes, R. Kennel, and M. P. Kazmierkowski, "Model predictive control - A simple and powerful method to control power converters," 2009 IEEE 6th Int. Power Electron. Motion Control Conf. IPEMC '09, vol. 56, no. 6, pp. 41–49, 2009, doi: 10.1109/IPEMC.2009.5289335.
- [10] D. M. C. Milbradt, G. V. Hollweg, P. J. D. de Oliveira Ewald, W. B. da Silveira, and H. A. Gründling, "A robust adaptive One Sample Ahead Preview controller for grid-injected currents of a grid-tied power converter with an LCL filter," *Int. J. Electr. Power Energy Syst.*, vol. 142, no. May, 2022, doi: 10.1016/j.ijepes.2022.108286.
- [11] D. Sgrò, S. A. Souza, F. L. Tofoli, R. P. S. Leão, and A. K. R. Sombra, "An integrated design approach of LCL filters based on nonlinear inductors for grid-connected inverter applications," *Electr. Power Syst. Res.*, vol. 186, no. May, p. 106389, 2020, doi: 10.1016/j.epsr.2020.106389.
- [12] X. Q. Guo, W. Y. Wu, and H. R. Gu, "Modeling and simulation of direct output current control for LCL-interfaced grid-connected inverters with parallel passive damping," *Simul. Model. Pract. Theory*, vol. 18, no. 7, pp. 946–956, 2010, doi: 10.1016/j.simpat.2010.02.010.
- [13] C. C. Gomes, A. F. Cupertino, and H. A. Pereira, "Damping techniques for grid-connected voltage source converters based on LCL filter: An overview," *Renew. Sustain. Energy Rev.*, vol. 81, no. 2018, pp. 116–135, 2018, doi: 10.1016/j.rser.2017.07.050.
- [14] C. Gurrola-Corral, J. Segundo, M. Esparza, and R. Cruz, "Optimal LCL-filter design method for grid-connected renewable energy sources," *Int. J. Electr. Power Energy Syst.*, vol. 120, no. 2020, pp. 1–14, 2020, doi: 10.1016/j.ijepes.2020.105998.
- [15] J. Zhao, W. Wu, Z. Shuai, A. Luo, H. S. H. Chung, and F. Blaabjerg, "Robust Control Parameters Design of PBC Controller for LCL-Filtered Grid-Tied Inverter," *IEEE Trans. Power Electron.*, vol. 35, no. 8, pp. 8102–8115, 2020, doi: 10.1109/TPEL.2019.2963200.
- [16] M. Dursun and M. K. Dosoglu, "LCL Filter Design for Grid Connected Three-Phase Inverter," *ISMSIT 2018 - 2nd Int. Symp. Multidiscip. Stud. Innov. Technol. Proc.*, no. 3, pp. 3–6, 2018, doi: 10.1109/ISMSIT.2018.8567054.
- [17] M. I. Solihin, L. F. Tack, and M. L. Kean, "Tuning of PID Controller Using Particle Swarm Optimization (PSO)," *Int. J. Adv. Sci. Eng. Inf. Technol.*, vol. 1, no. 4, p. 458, 2011, doi: 10.18517/ijaseit.1.4.93.
- [18] T. Adel and C. Abdelkader, "A Particle Swarm Optimization approach for optimum design of PID controller for nonlinear systems," in 2013 International Conference on Electrical Engineering and Software Applications, ICEESA 2013, 2013, pp. 1–4, doi: 10.1109/ICEESA.2013.6578478.
- [19] Y. Li, K. H. Ang, and G. C. Y. Chong, "PID Control System Analysis and Design: Problems, Remedies, and Future Directions," *IEEE Control Syst.*, vol. 26, no. 1, pp. 32–41, 2006, doi: 10.1109/MCS.2006.1580152.
- [20] H. Li, W. Wu, M. Huang, H. Shu-Hung Chung, M. Liserre, and F. Blaabjerg, "Design of PWM-SMC Controller Using Linearized Model for Grid-Connected Inverter with LCL Filter," *IEEE Trans. Power Electron.*, vol. 35, no. 12, pp. 12773–12786, 2020, doi: 10.1109/TPEL.2020.2990496.
- [21] M. B. Shadmand, R. S. Balog, and H. Abu-Rub, "Model predictive control of PV sources in a smart DC distribution system: Maximum power point tracking and droop control," *IEEE Trans. Energy Convers.*, vol. 29, no. 4, pp. 913–921, 2014, doi: 10.1109/TEC.2014.2362934.
- [22] A. Abu-Rmieleh and W. Garcia-Gabin, "A gain-scheduling model predictive controller for blood glucose control in type 1 diabetes," *IEEE Trans. Biomed. Eng.*, vol. 57, no. 10 PART 1, pp. 2478–2484, 2010, doi: 10.1109/TBME.2009.2033663.
- [23] M. Shadmand, R. S. Balog, and H. Abu Rub, "Maximum Power Point Tracking using Model Predictive Control of a flyback converter for photovoltaic applications," 2014 Power Energy Conf. Illinois, pp. 1–5, 2014, doi: 10.1109/peci.2014.6804540.
- [24] P. Cortes, A. Wilson, S. Kouro, J. Rodriguez, and H. Abu-Rub, "Model predictive control of multilevel cascaded H-bridge inverters," *IEEE Trans. Ind. Electron.*, vol. 57, no. 8, pp. 2691–2699, 2010, doi: 10.1109/TIE.2010.2041733.
- [25] M. B. Shadmand, M. Mosa, R. S. Balog, and H. A. Rub, "An improved MPPT technique for high gain DC-DC converter using model predictive control for photovoltaic applications," *Conf. Proc. - IEEE Appl. Power Electron. Conf. Expo. - APEC*, pp. 2993–2999, 2014, doi: 10.1109/APEC.2014.6803730.

## BIOGRAPHIES



**EKREM DEMİR** graduated from Sakarya University in Turkey in 2015 in the field of electrical and electronic engineering and received his M.Sc. He graduated from Karabuk University, Department of Electrical and Electronics Engineering in 2020. He has been working as a Research Assistant at Karabuk University, Department of Electrical and Electronics Engineering since 2018. His research interests include inverter topologies, converter topologies, PID control and model predictive control.





**OZAN GULBUDAK** received the B.Sc. and the M.Sc. degree in electrical engineering from Mersin University, Turkey in 2008 and 2010. He received Ph.D. degree from the University of South Carolina, Columbia, USA. Since 2017, he has been with Karabuk University, where is currently Assistant Professor. His research interests include model predictive control, development of control platforms based on FPGA, direct matrix converters, inverter topologies and motor drives.



**MUSTAFA GOKDAG** received the B.Sc. degree with Honor in electrical and electronics engineering from Fırat University, Turkey, in 2009, and the M.Sc. and Ph.D. degrees in electrical and electronics engineering from Karabuk University, Turkey, in 2011 and 2016 respectively. From 2009 to 2016, he was a Research Assistant with the department of electrical and electronics engineering in Karabuk University. Since 2016, he has been an Assistant Professor in same department. His research interests include modeling and control of dc-dc power converters and model predictive control of ac-dc, dc-ac, and ac-ac power converters for renewable and electrical drives.